

Climatological Estimates of Hourly Tornado Probability for the United States

MAKENZIE J. KROCAK

Cooperative Institute for Mesoscale Meteorological Studies, University of Oklahoma, and NOAA/OAR/National Severe Storms Laboratory, Norman, Oklahoma

HAROLD E. BROOKS

NOAA/OAR/National Severe Storms Laboratory, and the University of Oklahoma School of Meteorology, Norman, Oklahoma

(Manuscript received 18 August 2017, in final form 20 October 2017)

ABSTRACT

While there has been an abundance of research dedicated to the seasonal climatology of severe weather, very little has been done to study hazardous weather probabilities on smaller scales. To this end, local hourly climatological estimates of tornadic event probabilities were developed using storm reports from NOAA's Storm Prediction Center. These estimates begin the process of analyzing tornado frequencies on a subdaily scale.

Characteristics of the local tornado climatology are investigated, including how the diurnal cycle varies in space and time. Hourly tornado probabilities are peaked for both the annual and diurnal cycles in the plains, whereas the southeast United States has a more variable pattern. Areas that have similar total tornado threats but differ in the distribution of that threat are highlighted. Additionally, areas that have most of the tornado threat concentrated in small time frames both annually and diurnally are compared to areas that have a low-level threat at all times. These differences create challenges related to staffing requirements and background understanding of the tornado threat unique to each region.

This work is part of a larger effort to provide background information for probabilistic forecasts of hazardous weather that are meaningful over broad time and space scales, with a focus on scales broader than the typical time and space scales of the events of interest (including current products on the "watch" scale). A large challenge remains to continue describing probabilities as the time and space scales of the forecast become comparable to the scale of the event.

1. Introduction and background

Tornadoes cause large amounts of damage to life and property every year in the United States. There have been numerous attempts to quantify the climatological risk of these hazards; however, because of the nature of tornadoes being rare events everywhere, a large sample size is needed to produce accurate climatological estimates. Additionally, researchers also have to contend with inconsistent record keeping, which creates a trade-off between sample sizes and inconsistent reporting practices.

Many of the tornado climatological estimates are created using only parts of the total report database in an attempt to reduce the errors associated with it while also

maintaining a sufficient number of reports. Those studies that use only (E)F2 and greater reports (Concannon et al. 2000; Coleman and Dixon 2014) have found the maximum probability of tornado occurrence to be in an L-shaped pattern extending from Iowa down into Oklahoma and then east into Mississippi and Alabama. Some of the highest risk areas are located in the southeastern (SE) portions of the United States: the tornado threat tends to start in these areas in the beginning of the year and then move north during the summer before returning to the south in the fall and winter following the spatiotemporal shift in ingredients necessary for severe convective storms (Gensini and Ashley 2011). Another method discussed by Kelly et al. (1978) attempted to remove report bias from the record, while still retaining 80% of the reports. Report times were converted to mean solar time and then analyzed. Results showed that most violent

Corresponding author: Makenzie Krocak, makenzie.krocak@noaa.gov

DOI: 10.1175/WAF-D-17-0123.1

© 2018 American Meteorological Society. For information regarding reuse of this content and general copyright information, consult the [AMS Copyright Policy](#) (www.ametsoc.org/PUBSReuseLicenses).

tornadoes occur on outbreak days, except in the SE United States.

Throughout the literature, one common theme is the differences in climatological tornado patterns between the plains and the SE United States. The latter often sees a high number of nocturnal tornadoes, which is analyzed on a climatological scale in [Kis and Straka \(2010\)](#). Environmental data taken from model proximity soundings around nocturnal tornadoes revealed that environments commonly found in the fall and winter months in the SE United States (with low instability but substantial low-level vertical wind shear) often supported tornadic storms. This is significant because these environments were previously thought to be suboptimal for these types of storms. Other work (e.g., [Rasmussen and Blanchard 1998](#); [Rasmussen 2003](#); [Thompson et al. 2003](#)) also looked at environmental factors supportive of tornado reports, but focused on events associated with supercells [unlike the [Kis and Straka \(2010\)](#) study]. Deep-layer shear and convective available potential energy (CAPE) values were found to discriminate between tornadic and nontornadic environments, particularly in the plains.

Changes to the climatology of tornado occurrence throughout the latter half of the twentieth century have also been investigated. While [Verbout et al. \(2006\)](#) found an average of 18 “big tornado days” per year, which are defined as days having more than eight F1 or higher tornadoes, other studies including [Brooks et al. \(2014\)](#) and [Elsner et al. \(2015\)](#) found a decrease in the number of days per year with at least one (E)F1+ tornado report. Essentially, each day has a lower probability of a tornado occurring, but if tornadoes do occur, there is a higher probability of having multiple tornadoes. Therefore, the number of days with tornadoes has decreased over the last four decades, but the number of big tornado days (or outbreak days) has increased.

In addition to these findings, there are indications that interseasonal tornado climatology characteristics are also changing. [Tippett \(2014\)](#) used a tornado environment index to assess whether changes to the number of tornadoes per year are due to deviations in reporting practice or real atmospheric changes. Results showed that changes did occur to this index after 2000, indicating that there is now more volatility to U.S. tornado frequencies. While one year may have few reports, the next could be a record-high report year. Finally, [Long and Stoy \(2014\)](#) and [Lu et al. \(2015\)](#) both found that the peak in the tornado season is shifting to earlier in the year in the plains, which has implications for community resilience to these types of disasters.

A key challenge to protecting individuals from these events is describing the threat with enough specificity to

elicit some type of protective action. One way to include more specific information in forecasts is to add probabilistic information about the threat. The Storm Prediction Center (SPC) currently includes the probability of a severe event occurring within 40 km of a point in the convective outlook product. [Hitchens et al. \(2013\)](#) evaluated these probabilities and showed an increase in skill since the mid-1990s. The SPC also includes probabilities within the spatiotemporal bounds of watch products, which [Vescio and Thompson \(2001\)](#) examined. They found that adding probabilistic information was useful in highlighting the area of greatest threat within the watch.

As ensembles of convection-allowing models become operational, it becomes natural for probabilistic forecasts to replace traditional deterministic information. The recent NOAA initiative called the Forecasting a Continuum of Environmental Threats (FACETs) project aims to usher in a new forecasting paradigm with probabilistic information about hazardous weather threats on a range of scales. This includes forecasts on regional spatial scales more than a week out to neighborhood spatial scales just a few minutes before the event occurs. The project aims to transform the current dichotomous severe weather watch and warning system into one with a continuous stream of probabilistic hazardous weather information ([Rothfus et al. 2014](#)).

For the most part, the paradigm underlying the current severe weather forecasting system consists of three different forecasting periods. The first, and longest, are the convective outlooks, which are issued up to 8 days in advance and include 24-h (1200–1200 UTC) probabilities of severe weather threats up until the first day-1 issuance. The remaining convective outlooks are valid from issuance until 1200 UTC the next day. Convective outlooks are the only scheduled products; the rest of the products discussed are issued on an as-needed basis. The second level consists of mesoscale discussions (which contain the probability of a watch being issued) and watches. These products are valid upon issuance and usually last on the order of 2–8 h. The third level is the warning, which is also valid upon issuance, usually lasts less than 1 h, and does not contain any probabilistic information.

Climatological values of hazard threats have traditionally been calculated to correspond to the convective outlook period (e.g., [Brooks et al. 2003](#)). Our goal in this paper is to develop a subdaily climatology to provide tornadic probability information on finer time scales and show variations in hourly values by time of day, time of year, and location. We compare areas that have all of the threat concentrated in small time frames both annually and diurnally to areas that have a low-level threat at all times. These differences in distributions have implications

for all users, from community members and emergency managers to forecasters. In an effort to provide useful climatological information at a higher resolution, we developed this hourly climatology of tornado probabilities using similar methods to the work described by Brooks et al. (2003). Along with the climatological estimates, we discuss the implications of the differences in the distribution of tornado probabilities by region and how these differences play a role in region-specific disaster planning.

2. Data

In our study, storm reports from the SPC severe report database (Schaefer and Edwards 1999) were used to create the hourly climatological estimates. Reports are collected from National Weather Service offices, quality controlled to remove erroneous and duplicate reports, and then sent to the SPC where the times are then converted to central standard time. Reports between 1954 and 2015 were used because there are a number of changes that occurred in reporting practices during the earlier years of the severe weather report database (Doswell and Burgess 1988).

Similar to Verbout et al. (2006), the dataset used includes all (E)F1 and greater tornado reports (Doswell et al. 2009) between the years 1954 and 2015. Brooks et al. (2003) showed that while the number of tornado reports of any rating nearly doubled between the mid-1950s and the early 2000s, the number of tornado days (days where at least one tornado was reported somewhere in the United States) only rose 10%–15%. Other work has also shown that the number of strong and violent tornadoes remained relatively constant throughout the period (Schaefer and Schneider 2002). Additionally, when the dataset is restricted to only (E) F1+ tornadoes, there is no significant trend in the number of reports (Brooks et al. 2014). Given this lack of an increase in reports, we are reasonably confident that our calculated climatological estimates are robust.

3. Statistical treatment

This study uses report gridding and smoothing processes similar to other climatology work (e.g., Thom 1963; Brooks et al. 2003). Reports were assigned a grid point based on the location of the report (touchdown location for tornadoes) and the hour the report occurred. Locations were plotted on a Lambert conformal grid with approximately 80-km horizontal grid spacing. The grid is true at 39.8°N. These characteristics were chosen because they are similar to those currently used by forecasters in the SPC for convective outlook forecasts. Grid boxes that contained a report were assigned

the number one, with all other grid boxes assigned a zero. First, we created and examined climatological estimates for each year. This approach enabled statistical analysis of any combination of years, such as yearly or decadal averages. Next, yearly grids were wrapped such that 31 December and 1 January were adjacent to each other. Grids were smoothed after they were wrapped to ensure continuity within the beginning and ending year estimates. After smoothing the ones and zeros, these values are equivalent to the probability of a tornado occurring within the grid box in that hour.

Special attention was paid to non-leap years after the smoothing process was completed. While yearly grids for leap years contained 366×24 h, non-leap years were 1 day short of that. Therefore, a single day was inserted into the non-leap year grids after 28 February, and then hourly probabilities were linearly interpolated between corresponding hours on 28 February and 1 March. This additional step created yearly grids that were all the same size regardless of leap year status and allowed for analysis over the entire period.

To create consistent probabilities, the hourly gridded reports for each individual year were smoothed both spatially and temporally using nonparametric density estimation (Silverman 1986). We wanted to create yearly smoothed probability fields that still contained important information about the annual and diurnal tornado cycles. However, we also did not want large gradients in probability between hours or days. Further discussion of desirable qualities of climatological values can be found in Brooks et al. (2003). Once a smoothed field for each year was created, we analyzed different samples from the entire 62-yr set of smoothed probabilities.

For clarity, we will separate the description of the smoothing procedure into three parts. Beginning with the spatial treatment, grids were smoothed at each hour using a two-dimensional Gaussian filter:

$$P = \sum_{n=1}^N \frac{1}{2\pi\sigma^2} e^{-d^2/2\sigma^2}, \quad (1)$$

where P is the smoothed probability, N is the total number of grid boxes with events, d is the distance from the point location to the report location, and σ is the standard deviation of the Gaussian distribution, or the smoothing parameter. The standard deviation used for the spatial smoothing was 120 km.

Since this work focuses on the subdaily estimates of severe weather events, the temporal smoothing procedures become critical for the magnitudes of our final estimates. All values at the same time of the day were smoothed using a one-dimensional Gaussian filter with a 15-day standard deviation:

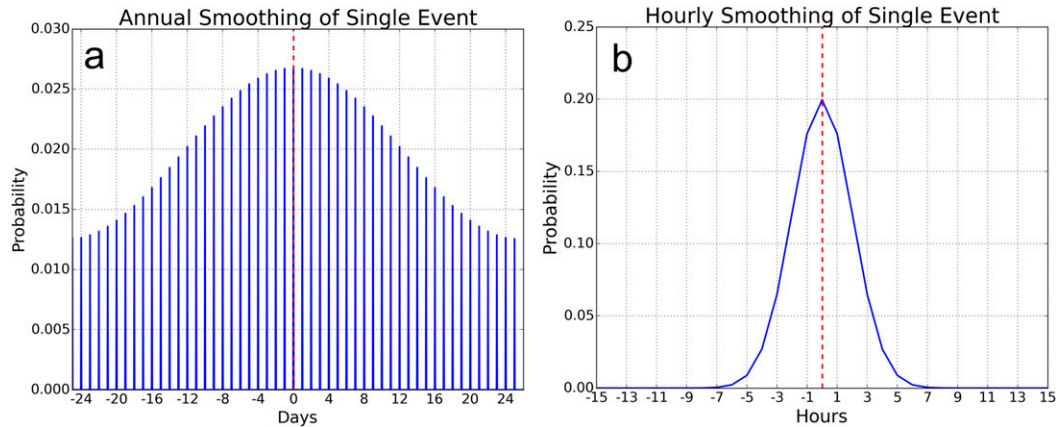


FIG. 1. Results of smoothing a single event using a Gaussian filter over the (a) annual and (b) daily cycles.

$$P = \sum_{n=1}^N \frac{1}{2\pi\sigma^2} e^{-t^2/2\sigma^2}. \quad (2)$$

For example, all 0000 UTC hour values were gathered and then smoothed with the 15-day smoothing parameter shown above, where t is the distance from the hour value being smoothed (Fig. 1a). The spatial and annual smoothing parameters (120 km and 15 days) were chosen to be consistent with previous climatological estimates (Brooks et al. 2003).

Since this work attempts to represent the annual and daily tornado probability cycles, there are a few desirable qualities that need to be preserved. We believe it is desirable that the annual values should change much slower than the daily values, as represented by the annual versus diurnal cycle. For example, values at 1400 UTC 15 May should be similar to values at 1400 UTC 16 May. However, these values should vary significantly from values at 0000 UTC on either day. To achieve these desirable qualities, hourly probabilities within the same day were smoothed using a 2-h smoothing parameter (Fig. 1b). The diurnal smoothing parameter was chosen for a number of different reasons. There are fewer reports overnight, highlighting the need for a smoothing method that would add information to these time frames without oversmoothing the low signal from the reports. Estimates using both a 1- and a 2-h smoothing parameter were analyzed (Fig. 2). The impact of the different smoothing values can be seen best in locations in the southeastern United States. The 2-h parameter produces a smoother field than the 1-h parameter and tends to produce fewer local extrema within the day, which we view as desirable. Heavier smoothers flatten the diurnal cycle even more and spread information over a large part of the day. We chose to use a simple filter with a single standard deviation at each step

and location because it is reasonably appropriate over almost all locations and times. While we understand there are times and locations where this choice is not appropriate, we have no way of knowing where and when those instances are a priori.

The reason for this multistep smoothing process was to ensure the creation of a seasonal tornado cycle, while also preserving the smaller-scale diurnal cycle. Again, it was important to represent both the annual and the daily cycles of these events so users have accurate and reliable background information. Mathematically, the steps can be combined, since the operations are commutative, but separating them out here makes the steps clearer. After grids for each year of reports were created and smoothed, long-term mean values were calculated for each location. This approach allowed for an overall hourly climatology to be analyzed, as well as changes throughout the 62-yr period.

4. Results

After the gridding and smoothing process of all (E)F1 and higher-rated tornadoes, the total climatological number of tornadoes per year was calculated for any point in the United States by simply adding all hourly probability values together (Fig. 3). Values in central Oklahoma and north Texas are similar to values in Mississippi and Alabama. However, these tornado probabilities are distributed differently based on the region of the United States. The hourly climatology, in particular, highlights important differences in how the tornado threat is distributed.

To better visualize the locations of annual and daily peaks in tornado probability, heat maps of all hours of the year were plotted for a number of locations.

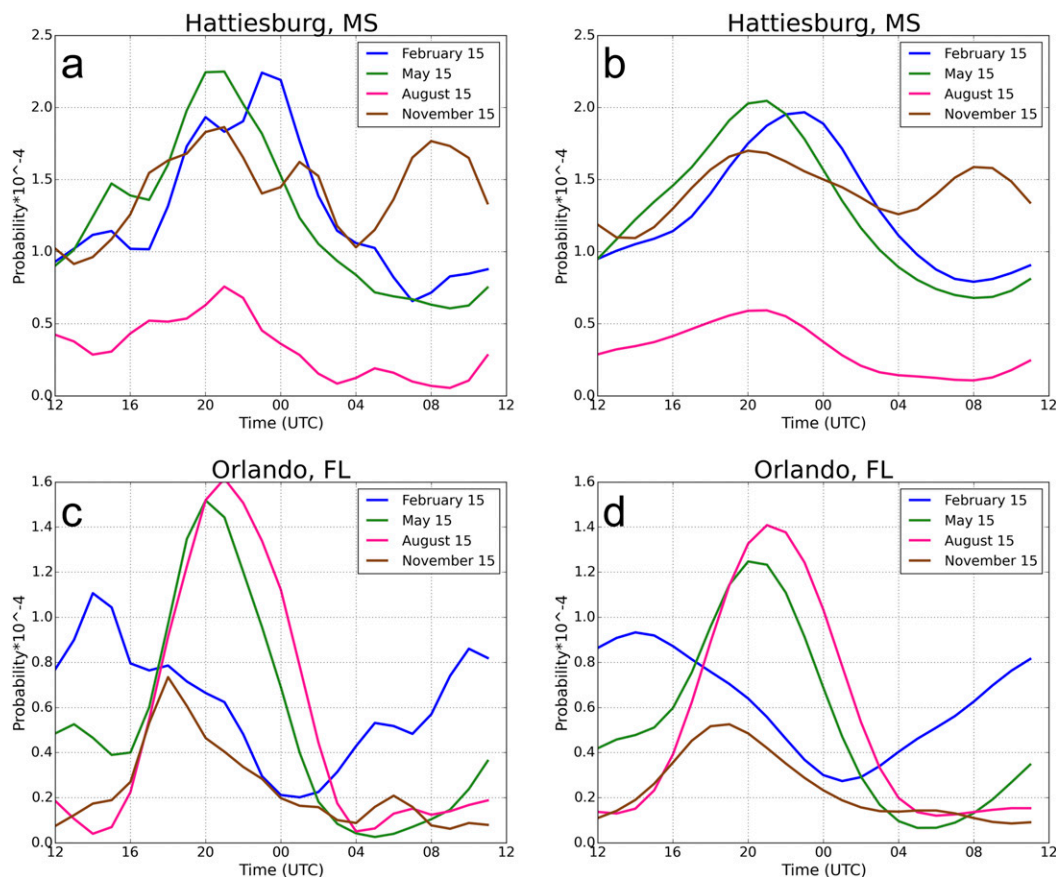


FIG. 2. Hourly tornado probability for (top) Hattiesburg and (bottom) Orlando, smoothed with (a),(c) 1- and (b),(d) 2-h parameters.

Norman, Oklahoma, and Huntsville, Alabama, show some of the greatest differences in the distribution (Fig. 4) and exemplify the differences between the tornado threats in the plains versus the SE United States. Norman shows a single, strong peak in April and May between the hours of 2000 and 0400 UTC. Beyond this time frame, probabilities are low, which indicates a specific, concentrated season and time of day during which tornadoes usually occur. In contrast, Huntsville has a relative maximum in probability in March and April from 2000 to 0400 UTC, but this maximum is only about 40% of the maximum in Norman. Additionally, overnight values around the peak in Huntsville remain at 40%–50% of the peak, whereas overnight values in Norman drop to about 10% of the peak value. These results indicate that the tornado threat is spread across a much broader time frame in the SE United States than it is in the plains.

In addition to the variability in diurnal tornado probability cycles across the United States, there is also variability in cycles throughout the year. The daily cycles of tornado probability for four different times of the

year are plotted for York, Nebraska; Columbus, Ohio; Lubbock, Texas; Hattiesburg, Mississippi; and Orlando, Florida (Fig. 5; locations shown in Fig. 3). Similar to what was seen in the heat maps for Norman and Huntsville, one of the most obvious differences between the five sites is the distinction between the plains locations and the SE U.S. locations. York, Columbus, and Lubbock all show a strong seasonal cycle, with May–June having the highest hourly probability values corresponding to the peak in hourly tornado probability (around 0.0008, 0.0003, and 0.0005, respectively, for the 15 May values) and peaks outside of this time period being lower in magnitude. Hattiesburg and Orlando do not show the same strong seasonal cycle. Many of the peaks throughout the different times of the year have similar magnitudes of probability, indicating weaker seasonal tornado cycles.

Along with the weak seasonal cycles, there are also weak daily cycles for the SE U.S. locations. While York, Columbus, and Lubbock all show a strong peak around 2000–0000 UTC during the warm season with low probabilities outside of the peak, Hattiesburg and

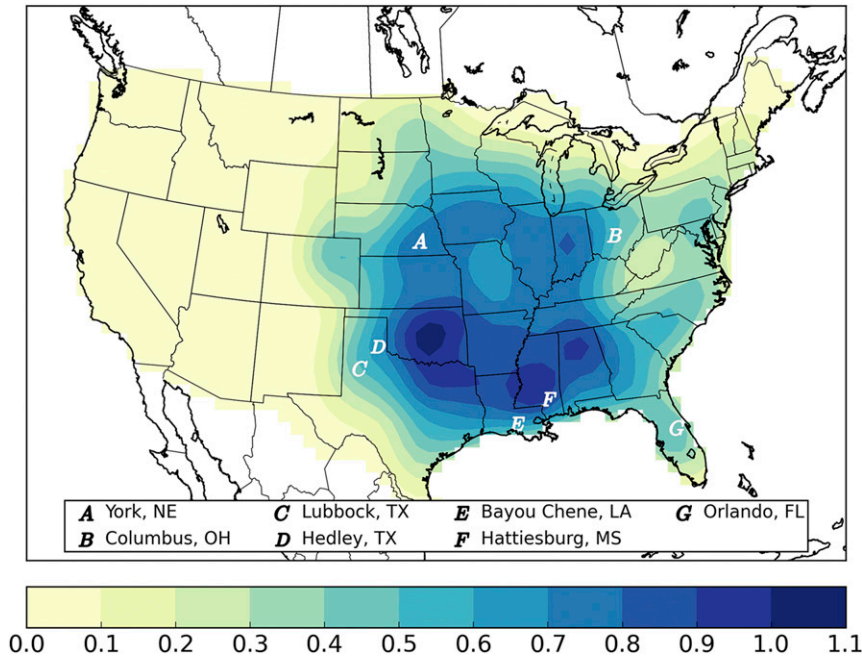


FIG. 3. The total number of tornadoes per year for every grid point across the United States.

Orlando do not have the same pattern. Probabilities outside of the peak remain relatively high, indicating the diurnal cycle does not play as strong of a role in tornado frequency in the SE United States as compared to the plains.

5. Possible applications

There are many benefits that come from having high-resolution climatological values for tornado occurrences. Small-scale patterns that were not previously

highlighted can now be visualized by region and time of day or year. In this section, we explore a few of the means by which we can examine these patterns.

The most notable difference in tornado probabilities between the SE United States and the plains is in the concentration of higher probability values. One method of visualizing the concentrations within the annual and diurnal cycles is to plot the annual cycle for each hour of the day (Fig. 6). This information was plotted for Hedley, Texas, and Bayou Chene, Louisiana (locations shown in Fig. 3). These two locations were chosen

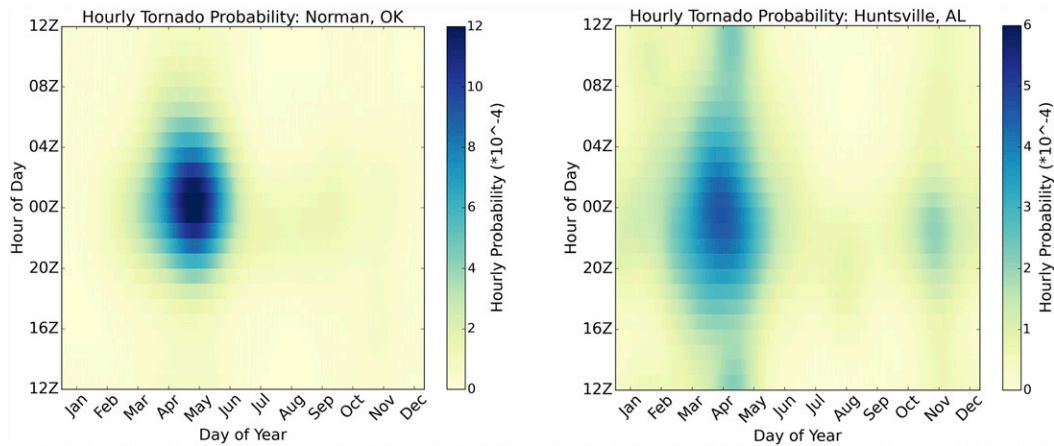


FIG. 4. Heat maps of tornado probability for Norman and Huntsville. Note the color bars are different. Each day is represented by a column and each hour by a different row.

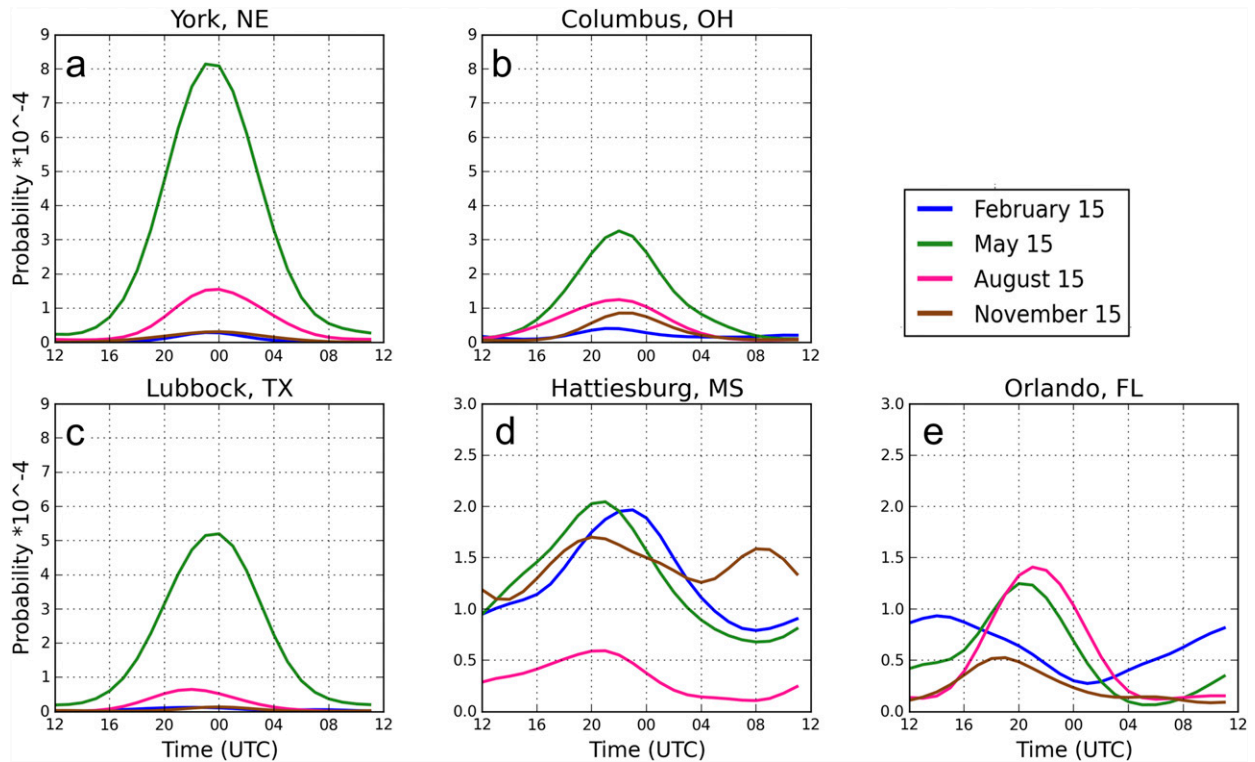


FIG. 5. Daily cycles of tornado probability in York, Columbus, Lubbock, Hattiesburg, and Orlando for four different times of the year. Note the two different vertical scales. The different colors represent the different times of the year (15 Feb, May, Aug, and Nov).

because the annual numbers of tornadoes for Hedley and Bayou Chene are similar (0.668 and 0.684, respectively). However, the distribution of that total threat is anything but. Hedley clearly has an annual peak in probability around day 140 (19 May), whereas Bayou Chene has no distinct peak. One could argue that there is a relative peak around day 125 (4 May), but this peak is around 25% of the magnitude of the peak in Hedley. To counter this high-amplitude peak in Hedley, the tornado probabilities outside of days 75–200 (15 March–18 July) are close to zero. This is not the case in Bayou Chene, where probabilities remain high relative to the peak for the entire year.

In addition to the lack of an annual cycle in Bayou Chene, there is also a weak daily cycle. The largest range in hourly tornado probabilities on a single day is about 0.5 of the largest value, whereas the largest range in Hedley is about 0.9 of the largest value. This finding is exemplified by the spacing of the hourly lines. These lines are widely spread in May in Hedley, which is not the case for any point during the year in Bayou Chene, where all 24 lines are much closer in magnitude.

The drastic differences in the distribution of nearly identical total annual tornadoes exemplify the challenges many forecasters face in the SE United States.

For example, a forecaster working on a tornado forecast for the middle of May in Hedley would likely be able to identify a 4–6-h period when tornadoes were most likely to occur without seeing any information about the synoptic setup or environmental parameters. In contrast, this would be very difficult for forecasters in Bayou Chene to do because the climatological hourly tornado probabilities are similar in magnitude for every hour during the month of May (and the entire year). These two sets of forecasters are working under different background climatologies, which pose different challenges to creating a forecast.

The different background climatologies could also lead to emergency managers and communities needing different disaster plans. Hedley residents are unlikely to experience a tornado in February at 0800 local time, but this is much more likely to happen in Bayou Chene. Those in Hedley might have a single disaster plan for all tornadoes because nearly all of the events they experience are in the afternoon during the late spring and early summer months. Those in Bayou Chene might need multiple disaster plans for tornadoes: one for winter events, one for spring events, one for school hours, and one for rush hour traffic. This relatively low risk spread out over a broad temporal range coupled with other

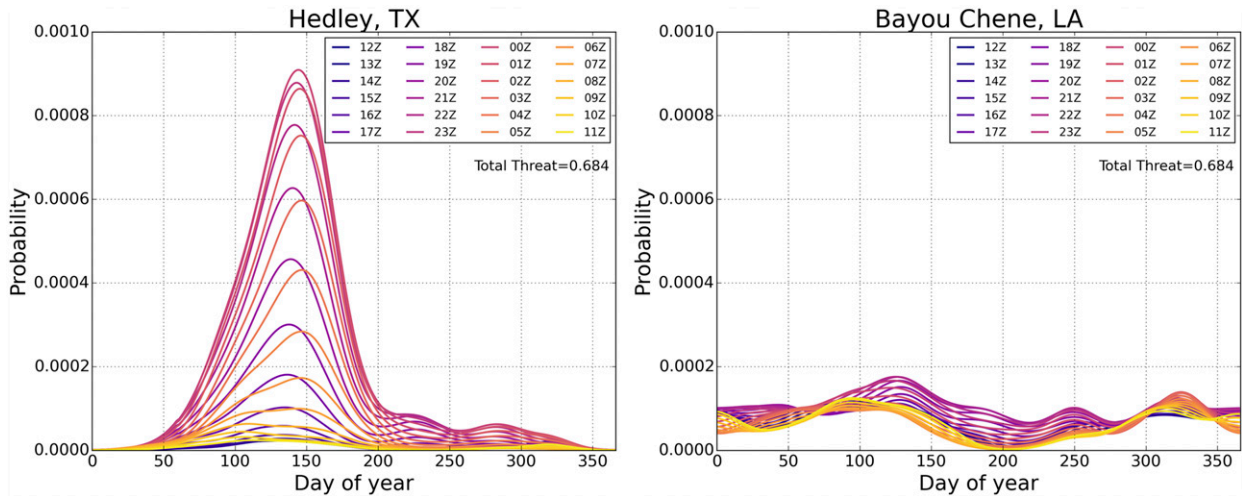


FIG. 6. Hourly tornado probabilities at corresponding hours for each day of the year for Hedley and Bayou Chene. Both graphs have 24 different lines, one for each hour when the hourly tornado probability during that hour for each day of the year was plotted. The total numbers of annual tornadoes are nearly identical for both locations.

demographic factors leads to the SE United States being particularly vulnerable to tornadic events (Ashley 2007). As meteorologists, it is imperative that we ensure people understand their threat, whether that be concentrated in a few days and hours, or spread out over broader time frames. Ultimately, the differences in both the annual and daily cycles of climatological tornado risks require both scientists and communicators to be aware of how the risk at their location impacts residents and property.

After examining the concentrations of diurnal cycles across the country, the next step was to find when the most peaked times occurred at each location. Therefore, the start time of the 4-h period with the highest sum of probabilities was plotted for each location (Fig. 7). The general pattern shows an earlier start time to the 4-h period on the East Coast than in the central plains. Start times in the eastern part of the country are as early as 1800 or 1900 UTC, whereas most of the start times in the plains are between 2100 and 2300 UTC. The differences in timing are likely related to the differing strengths of the capping inversion (“cap”) in these two areas. The cap in the plains is usually stronger than that in the SE United States, causing storms to initiate later in the afternoon. This then leads to severe weather reports and tornadoes occurring later in the plains than in the SE United States. These results again highlight the important differences between the tornado probabilities in the plains versus the probabilities in the SE United States. The maximum period in the plains is generally during the late evening hours, after most people have gone home from work or school. The SE United States has to respond to these events at a variety of times, many of

which have high traffic volumes. These are important differences to understand so that forecasters and emergency responders can work together to make region-specific disaster plans.

The high-resolution probability estimates also allow for much more tailored tornado threat estimates based on location and time frame. One example of this is the fraction of total annual tornadoes that occur during the school day (Fig. 8). This proportion was calculated as 5/7 (since children are in school 5 of 7 days in a week) of the sum of the hourly tornado probabilities that occur between 0700 and 1600 local time between 15 August and 15 June. There is a relative maximum in school day tornadoes in southern Alabama, southern Georgia, and Florida. More than 25% of all tornadoes occur during the school day in these areas, whereas areas in North Dakota experience less than 5% of their total tornadoes occurring during the school day. Proportions are higher where the daily and annual tornado cycles are less peaked, or where the peak occurs during the school day. The width of the tornado peak also manifests itself in these results. Those areas with a wider peak will have higher school day tornado occurrence, where areas with a lower width will have fewer tornadoes occur during the school day, especially if the peak is in the late evening.

These results have major implications for how these schools prepare for such disasters. Schools in the upper Midwest tend to have tornado drills once or twice during the school year. While this may be sufficient for an area that sees few tornadoes (and even fewer during school hours), other areas with a higher overall tornado risk and a higher number of tornadoes during

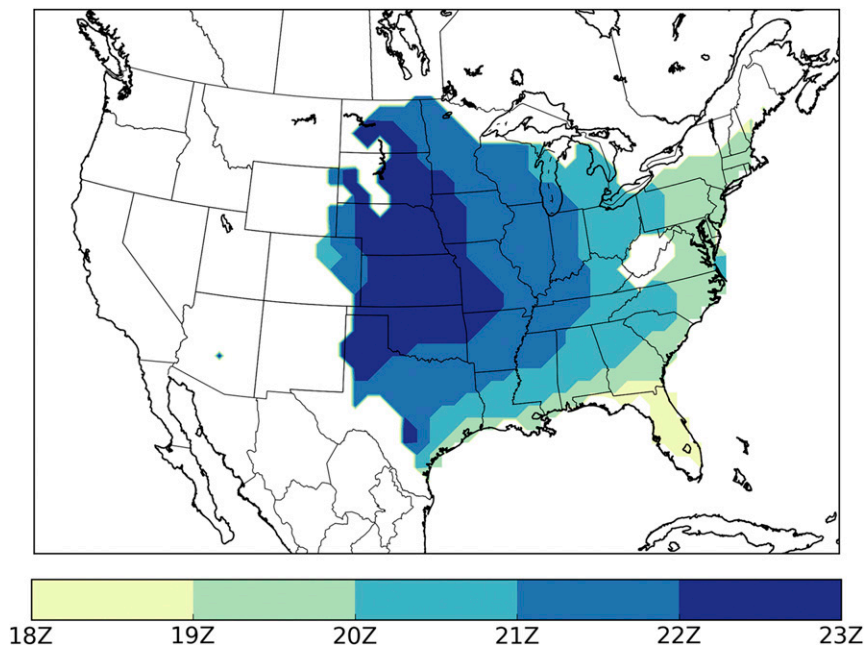


FIG. 7. Start time of the 4-h period that captures the highest fraction of tornado reports for every location across the country. Note the calculation was only done for points with greater than 40 reports over the 1954–2015 period.

school hours would likely need to have more frequent drills to keep both students and administrators aware of what protective actions need to be taken during the event of a tornado with children in the building.

Additionally, school dismissal on severe weather days has become a topic of discussion in many areas that see a higher tornado threat in the spring (Van Meter and Dixon 2014). These climatological estimates are

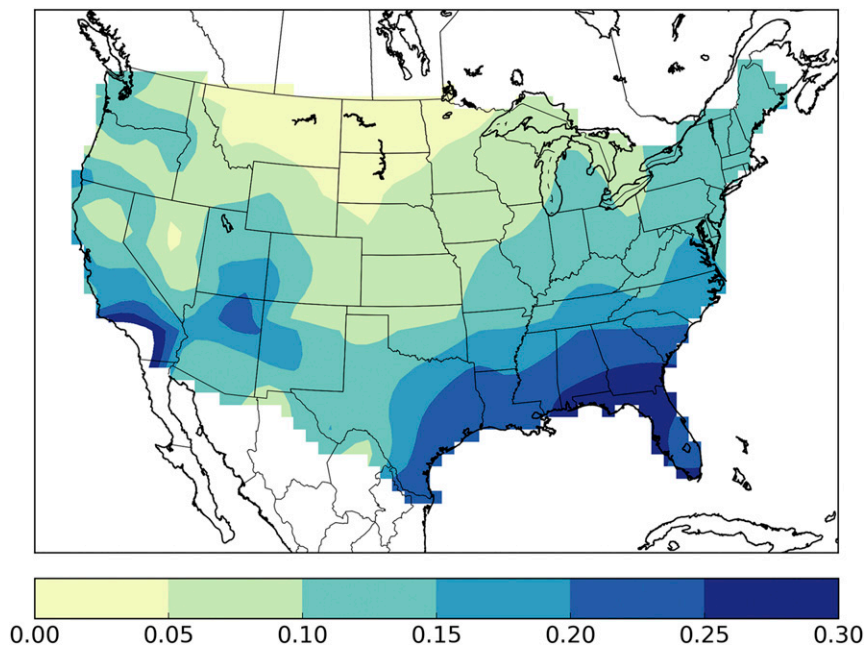


FIG. 8. The fraction of total annual tornadoes that occur during the school day, which is defined as hours of the work week between 0700 and 1600 local time between 15 Aug and 15 Jun.

able to provide insight as to which areas are more vulnerable to school day tornadoes and which ones are not, potentially decreasing the rate of over-dismissals in those areas less prone to these events.

6. Conclusions

An hourly climatology was developed for (E)F1 and greater tornadoes using 62 years' worth of tornado reports. All reports were gridded onto an 80-km grid by assigning all boxes with a report a one and all other boxes a zero. Grids were then smoothed spatially using a Gaussian filter with a 120-km standard deviation. Temporally, corresponding hours on each day were first smoothed with a 15-day standard deviation, and then adjacent hours were smoothed using a 2-h standard deviation. This entire process was done to ensure that the annual cycle of events was represented without over-smoothing the diurnal cycle. This resulted in adjacent daily sums of probabilities being nearly identical, and adjacent hourly probabilities differing with the diurnal cycle. The main goal of this work was to begin to understand the differences in the subdaily distributions as compared to the annual distributions of tornadic events.

Total annual tornado risks were found to peak in Oklahoma, as well as in the Mississippi and Alabama areas. However, while the total number of annual tornadoes was similar, the distribution of those tornadoes was different. While the plains have both a peaked annual cycle as well as a peaked diurnal cycle, the southeastern portion of the United States has a different climatological risk of tornadoes. Neither the annual cycle nor the diurnal cycle is peaked; probabilities are variable during all hours of the day and at all times of the year. This variability impacts planning decisions for both forecasters and for emergency managers, including staffing and scheduling decisions. Community members also need to be prepared to take action at inconvenient times or locations (i.e., at school, work, or during the night, etc.).

This hourly climatology begins the process of understanding the patterns and dependencies of tornadic events on a subdaily scale. The results show how both the annual and the diurnal cycles vary in space and time, which has implications for how forecasters could utilize the background probabilities of these events. Finally, these hourly tornado frequencies show that mitigation procedures need to be specific to the threat for each region of the United States.

Acknowledgments. This work originated in part from an M.S. thesis in the School of Meteorology at the University of Oklahoma. Funding was provided in part

by NOAA's Office of Weather and Air Quality through the U.S. Weather Research Program and by NOAA/Office of Oceanic and Atmospheric Research under NOAA–University of Oklahoma Cooperative Agreement NA11OAR4320072, U.S. Department of Commerce. The scientific results and conclusions, as well as any views or opinions expressed herein, are those of the authors and do not necessarily reflect the views of NOAA or the Department of Commerce.

REFERENCES

- Ashley, W. S., 2007: Spatial and temporal analysis of tornado fatalities in the United States: 1880–2005. *Wea. Forecasting*, **22**, 1214–1228, <https://doi.org/10.1175/2007WAF2007004.1>.
- Brooks, H. E., C. A. Doswell III, and M. P. Kay, 2003: Climatological estimates of local daily tornado probability for the United States. *Wea. Forecasting*, **18**, 626–640, [https://doi.org/10.1175/1520-0434\(2003\)018<0626:CEOLDT>2.0.CO;2](https://doi.org/10.1175/1520-0434(2003)018<0626:CEOLDT>2.0.CO;2).
- , G. W. Carbin, and P. T. Marsh, 2014: Increased variability of tornado occurrence in the United States. *Science*, **346**, 349–352, <https://doi.org/10.1126/science.1257460>.
- Coleman, T. A., and P. G. Dixon, 2014: An objective analysis of tornado risk in the United States. *Wea. Forecasting*, **29**, 366–376, <https://doi.org/10.1175/WAF-D-13-00057.1>.
- Concannon P. R., Brooks, H. E., and C. A. Doswell III, 2000: Climatological risk of strong and violent tornadoes in the United States. *Second Symp. on Environmental Applications*, Long Beach, CA, Amer. Meteor. Soc., 9.4, https://ams.confex.com/ams/annual2000/techprogram/paper_6471.htm.
- Doswell, C. A., III, and D. W. Burgess, 1988: On some issues of United States tornado climatology. *Mon. Wea. Rev.*, **116**, 495–501, [https://doi.org/10.1175/1520-0493\(1988\)116<0495:OSIOUS>2.0.CO;2](https://doi.org/10.1175/1520-0493(1988)116<0495:OSIOUS>2.0.CO;2).
- , H. E. Brooks, and N. Dotzek, 2009: On the implementation of the enhanced Fujita scale in the USA. *Atmos. Res.*, **93**, 554–563, doi:10.1016/j.atmosres.2008.11.003.
- Elsner, J. B., S. C. Elsner, and T. H. Jagger, 2015: The increasing efficiency of tornado days in the United States. *Climate Dyn.*, **45**, 651–659, <https://doi.org/10.1007/s00382-014-2277-3>.
- Gensini, V., and W. Ashley, 2011: Climatology of potentially severe convective environments from the North American Regional Reanalysis. *Electron. J. Severe Storms Meteor.*, **6** (8), <http://www.ejssm.org/ojs/index.php/ejssm/article/viewArticle/85>.
- Hitchens, N. M., H. E. Brooks, and M. P. Kay, 2013: Objective limits on forecasting skill of rare events. *Wea. Forecasting*, **28**, 525–534, <https://doi.org/10.1175/WAF-D-12-00113.1>.
- Kelly, D. L., J. T. Schaefer, R. P. McNulty, C. A. Doswell III, and R. F. Abbey, 1978: An augmented tornado climatology. *Mon. Wea. Rev.*, **106**, 1172–1183, [https://doi.org/10.1175/1520-0493\(1978\)106<1172:AATC>2.0.CO;2](https://doi.org/10.1175/1520-0493(1978)106<1172:AATC>2.0.CO;2).
- Kis, A. K., and J. M. Straka, 2010: Nocturnal tornado climatology. *Wea. Forecasting*, **25**, 545–561, <https://doi.org/10.1175/2009WAF2222294.1>.
- Long, J. A., and P. C. Stoy, 2014: Peak tornado activity is occurring earlier in the heart of “Tornado Alley.” *Geophys. Res. Lett.*, **41**, 6259–6264, <https://doi.org/10.1002/2014GL061385>.
- Lu, M., M. Tippet, and U. Lall, 2015: Changes in the seasonality of tornado and favorable genesis conditions in the central United States. *Geophys. Res. Lett.*, **42**, 4224–4231, <https://doi.org/10.1002/2015GL063968>.

- Rasmussen, E. N., 2003: Refined supercell and tornado forecast parameters. *Wea. Forecasting*, **18**, 530–535, [https://doi.org/10.1175/1520-0434\(2003\)18<530:RSATFP>2.0.CO;2](https://doi.org/10.1175/1520-0434(2003)18<530:RSATFP>2.0.CO;2).
- , and D. O. Blanchard, 1998: A baseline climatology of sounding-derived supercell and tornado forecast parameters. *Wea. Forecasting*, **13**, 1148–1164, [https://doi.org/10.1175/1520-0434\(1998\)013<1148:ABCOSD>2.0.CO;2](https://doi.org/10.1175/1520-0434(1998)013<1148:ABCOSD>2.0.CO;2).
- Rothfus L., C. Karstens, and D. Hilderband, 2014: Next-generation severe weather forecasting and communication. *Eos, Trans. Amer. Geophys. Union*, **95**, <https://eos.org/project-updates/next-generation-severe-weather-forecasting-communication>.
- Schaefer, J. T., and R. Edwards, 1999: The SPC tornado/severe thunderstorm database. Preprints, *11th Conf. on Applied Climatology*, Dallas, TX, Amer. Meteor. Soc., 603–606.
- , and R. S. Schneider, 2002: The robustness of tornado hazard estimates. *Third Symp. on Environmental Applications*, Orlando, FL, Amer. Meteor. Soc., 4.2, <https://ams.confex.com/ams/pdfpapers/27694.pdf>.
- Silverman, B. W., 1986: *Density Estimation for Statistics and Data Analysis. Monographs on Statistics and Applied Probability*, No. 26, Chapman and Hall, 175 pp.
- Thom, H. C. S., 1963: Tornado probabilities. *Mon. Wea. Rev.*, **91**, 730–736, [https://doi.org/10.1175/1520-0493\(1963\)091<0730:TP>2.3.CO;2](https://doi.org/10.1175/1520-0493(1963)091<0730:TP>2.3.CO;2).
- Thompson, R. L., R. Edwards, J. A. Hart, K. L. Elmore, and P. M. Markowski, 2003: Close proximity soundings within supercell environments obtained from the Rapid Update Cycle. *Wea. Forecasting*, **18**, 1243–1261, [https://doi.org/10.1175/1520-0434\(2003\)018<1243:CPSWSE>2.0.CO;2](https://doi.org/10.1175/1520-0434(2003)018<1243:CPSWSE>2.0.CO;2).
- Tippett, M. K., 2014: Changing volatility of U.S. annual tornado reports. *Geophys. Res. Lett.*, **41**, 6956–6961, <https://doi.org/10.1002/2014GL061347>.
- Van Meter, J. A., and P. G. Dixon, 2014: Early dismissals in public schools on potential severe weather days. *Nat. Hazards*, **73**, 1609–1624, <https://doi.org/10.1007/s11069-014-1162-z>.
- Verbout, S. M., H. Brooks, L. M. Leslie, and D. M. Schultz, 2006: Evolution of the U.S. tornado database: 1954–2003. *Wea. Forecasting*, **21**, 86–93, <https://doi.org/10.1175/WAF910.1>.
- Vescio, M. D., and R. L. Thompson, 2001: Subjective tornado probability forecasts in severe weather watches. *Wea. Forecasting*, **16**, 192–195, [https://doi.org/10.1175/1520-0434\(2001\)016<0192:FSFSTP>2.0.CO;2](https://doi.org/10.1175/1520-0434(2001)016<0192:FSFSTP>2.0.CO;2).